

INTRODUCTION: 61156 is a tough, medium gray, poikilitic impact melt rock that has been thermally metamorphosed. Macroscopically the rock is blocky and angular; few clasts are apparent (Fig. 1). Metal spherules and small vugs (<0.5 mm) are inhomogeneously distributed throughout the rock. There are many zap pits on the “lunar up” surface, few on other surfaces. This sample was collected 25 m northeast of Plum Crater.



FIGURE 1. 61156,0. S-72-38391.

PETROLOGY: Petrographic information is given by Albee et al. (1973), Simonds et al. (1973), and the Apollo 16 Lunar Sample Information Catalog (1972). Haggerty (1973) provides detailed microprobe analyses and descriptions of armalcolite and other oxides. Meyer et al. (1974) determined trace elements in plagioclase xenocrysts by ion microprobe. Metal compositions from an anorthositic clast and the poikilitic host are reported by Hewins and Goldstein (1975a).

61156 is a fine-grained, meta-poikilitic rock with several small (50-200 μm) plagioclase and pyroxene xenocrysts and at least one large (>10 mm) clast of anorthositic breccia. Modal data are presented by Albee et al. (1973) and the Apollo 16 Lunar Sample Information Catalog (1972) and reproduced here as Table 1. In the poikilitic host, mineral grains are anhedral and granular (Fig. 2) suggesting that the rock has undergone a period of extensive subsolidus annealing. Two types of poikilitic texture are randomly distributed throughout the rock. Most commonly, anhedral orthopyroxene oikocrysts (up to ~1 mm, averaging ~100 μm) enclose small, rounded, elongate to equant plagioclase crystals (20-50 μm). Pyroxene oikocrysts, however, are not as abundant in 61156 as in most of the other Apollo 16 poikilitic rocks. The second, less common poikilitic texture in this rock is characterized by an interlocking network of anhedral plagioclase grains (usually <50 μm) intergrown with small, equant grains of olivine and (rarely) high-Ca pyroxene (up to ~50 μm). Many of these mafic grains are optically continuous over an area generally <0.5 mm. Olivine and high-Ca pyroxene are not included within the orthopyroxene oikocrysts. K-rich patches are scattered throughout the rock but are never found within oikocrysts. Minerals are homogeneous and largely equilibrated (Fig. 3). Ridley and Adams (1976) calculate a temperature of equilibration of 1010°C for coexisting olivine and augite.

A wide variety of opaque and other accessory phases occur within the poikilitic portions of 61156, including ilmenite, armalcolite, Cr-spinel, rutile, baddelyite, metal, troilite and schreibersite. Oxides often form complex associations, probably representing the decomposition of some pre-existing oxide phase (Albee et al., 1973; Haggerty, 1973). Ilmenite plates are apparently not related to the development of oikocrysts. Metal occurs principally as 100-400 μm globules and is very homogeneous in composition (Fig. 4).

Xenocrysts of plagioclase and low-Ca pyroxene account for ~15% of the rock. Many of these plagioclase clasts have calcic cores (An_{95-97}) rimmed by overgrowths of the same composition as in the poikilitic host (An_{87-93}). Trace elements in plagioclase clasts as determined by ion microprobe (Meyer et al., 1974) are presented in Table 2. Ba in these clasts is significantly below the initial Ba expected by in situ crystallization.

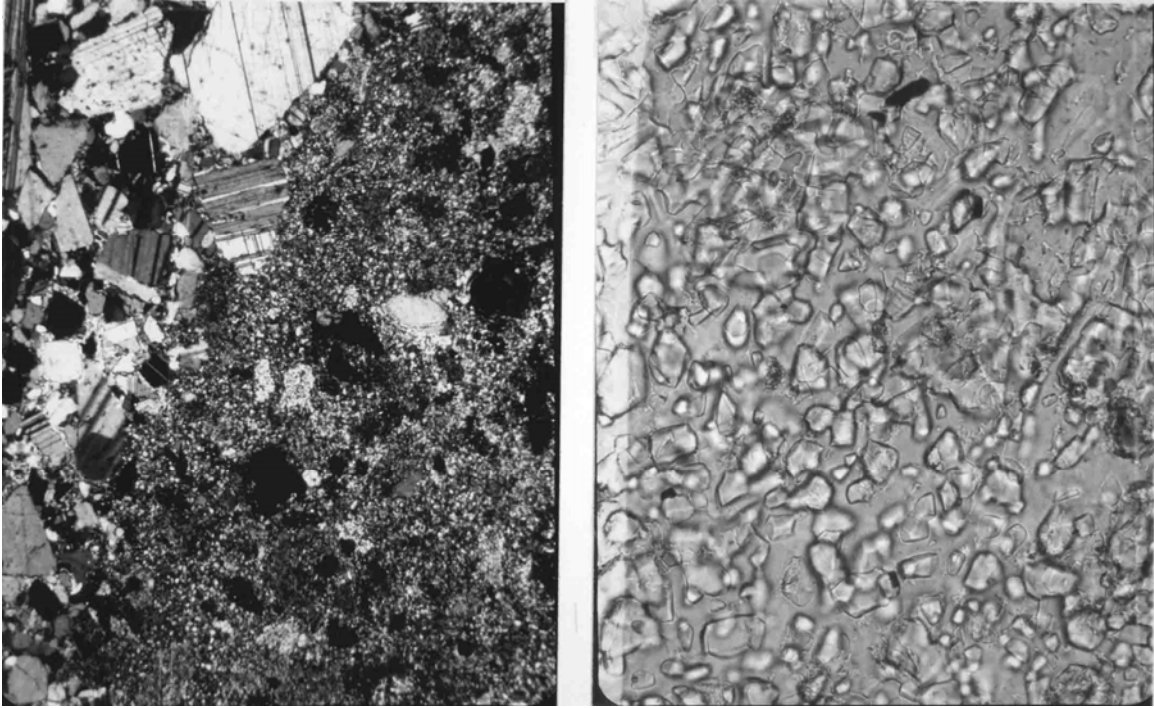


FIGURE 2. 61156,30.
 a) General view, xpl. Width 2 mm.
 b) Poikilitic area, ppl. Width 0.2 mm.

TABLE 1. Modal data for 61156.

	61156,5 (1300 pts; Apollo 16 Lunar Sample Information Catalog,1972)	61156,31 (1990 pts; Albee et al., 1973)	
		vol%	wt%
<u>orthopyroxene</u>	25.9	20.6	23.0
<u>oikocryst</u>	18.4		
<u>xenocryst</u>	7.5		
<u>plagioclase</u>	59.5	62.1	55.4
in oikocrysts	15.0		
surrounding olivine	38.0		
<u>xenocryst</u>	6.5		
<u>olivine</u>	11.7	10.2	12.9
<u>high-Ca pyroxene</u>		5.1	5.6
<u>metal</u>	1.0	0.3	0.9
<u>other opaques</u>	1.9	0.6	1.2
<u>phosphates</u>		0.3	0.3
<u>K-rich interstices</u>		0.6	0.5

TABLE 2. Trace elements in plagioclase xenocrysts in 61156.

Na ₂ O	0.39 wt%
Li	5
Mg	400
K	760
Ti	110
Sr	150
Ba	18

All data in ppm except as noted (from Meyer et al., 1974)

At least one large (>10 mm) clast of anorthositic breccia is also found in 61156. It consists of angular, well-twinned plagioclase (An₉₅; up to 1 mm) which has been coarsely crushed. Interstitial mafics are rare but, where present, tend to show a poikilitic texture; around smaller plagioclase grains within the clast. The clast-matrix boundary is irregular with matrix sometimes penetrating along grain boundaries of the clast. Metal in the clast is of the same composition as that in the poikilitic host (Fig. 4) (Hewins and Goldstein, 1975a).

CHEMISTRY: Major and trace element analyses are given by Hubbard et al. (1973), Wanke et al. (1974) and LSPET (1973). Albee et al. (1973) calculated major element bulk composition based on a mode and mineral analyses. Eldridge et al. (1973) provide data on natural and cosmogenic radionuclides. Rb, Sr and U, Th, Pb data are presented by Nyquist et al. (1973) and Tera et al. (1974) respectively.

Compositionally, 61156 is more similar to Apollo 16 basaltic melt rocks than to the other poikilitic melt rocks. It is more aluminous than most other poikilitic rocks (Table 3), plotting on the plagioclase-spinel cotectic in the system olivine-anorthite-silica (Fig. 5). Rare earth elements (Fig. 6) are moderately enriched over local soils but are significantly less than in the KREEP-rich poikilitic rocks such as 62235 and 60315. Siderophiles indicate a significant, though variable, meteoritic content (Table 3). This variation in levels of siderophiles is almost certainly due to the inhomogeneous distribution of metal.

RADIOGENIC ISOTOPES AND GEOCHRONOLOGY: Nyquist et al. (1973) report whole rock Rb-Sr isotopic data. Tera et al. (1974) provide whole rock Rb-Sr and U-Th-Pb isotopic data.

The data are summarized in Table 4. Notable are the old model ages calculated from Rb-Sr systematics. U-Pb isotopes do not show such old model ages. The whole rock analysis of Tera et al. (1974) is within error of concordia at 4.24 b.y.

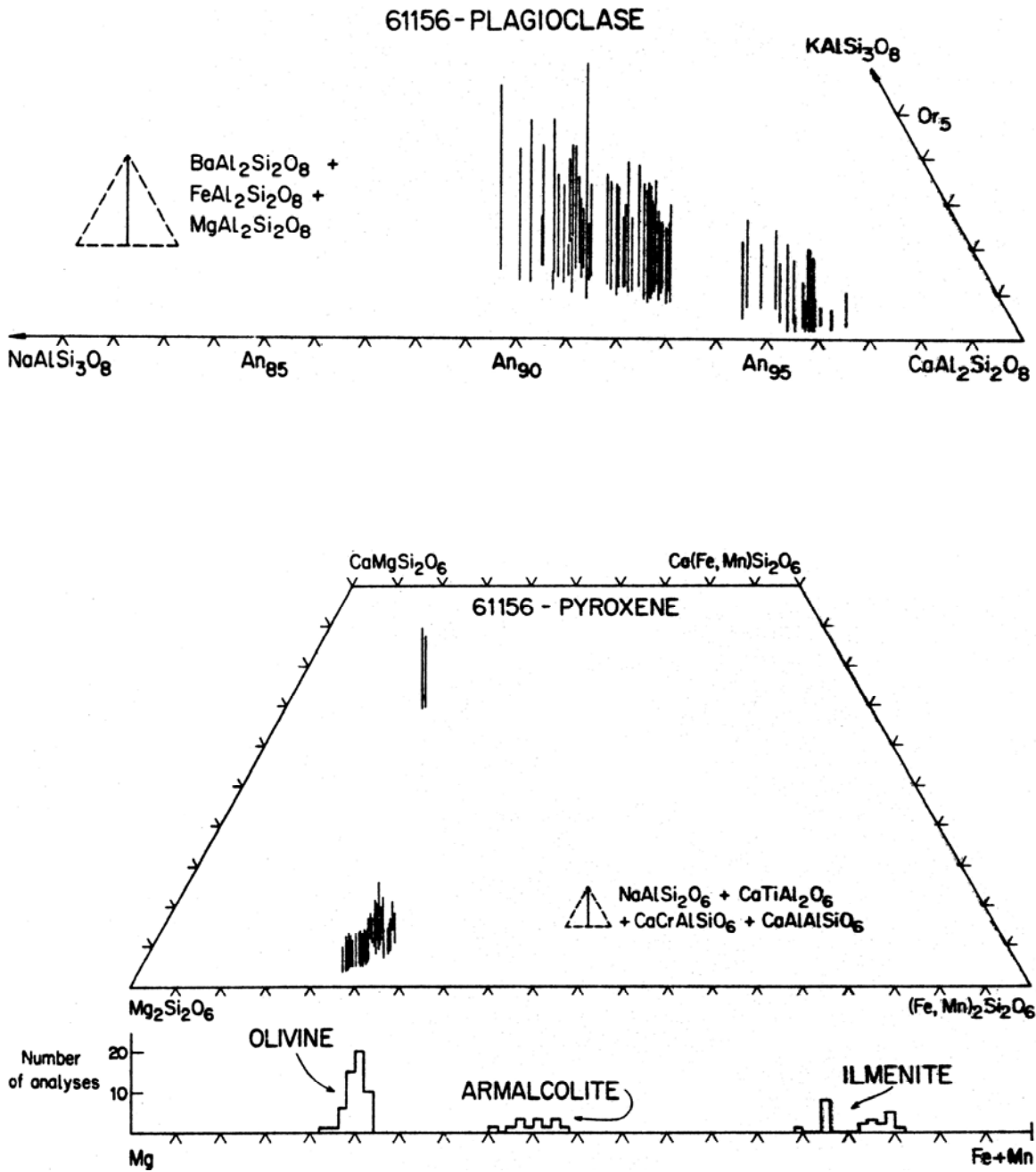


FIGURE 3. Mineral compositions, from Albee et al. (1973).

MICROCRATERS: Neukum et al. (1973) provide size-frequency data (Fig. 7). They conclude that the surface of 61156 is in production.

PHYSICAL PROPERTIES: Intrinsic and remanent magnetic parameters were measured on two splits of 61156 by Nagata et al. (1974) using hysteresis and AF-demagnetization techniques. They find no significant residue of NRM after 150 Oe-rms demagnetization. Greater than 90% of the metal in 61156 is kamacite with 4-6% Ni. Schwerer and Nagata (1976) determined size distribution data for metallic particles in the 0.003-0.15 μm (30-150 \AA) size range using magnetic granulometry. The mean grain size of fine-grained metal in this rock is 37 \AA .

Huffman et al. (1974) present Mossbauer and magnetic analyses of the same two splits studied by Nagata et al. (1974). These results are summarized in Table 5.

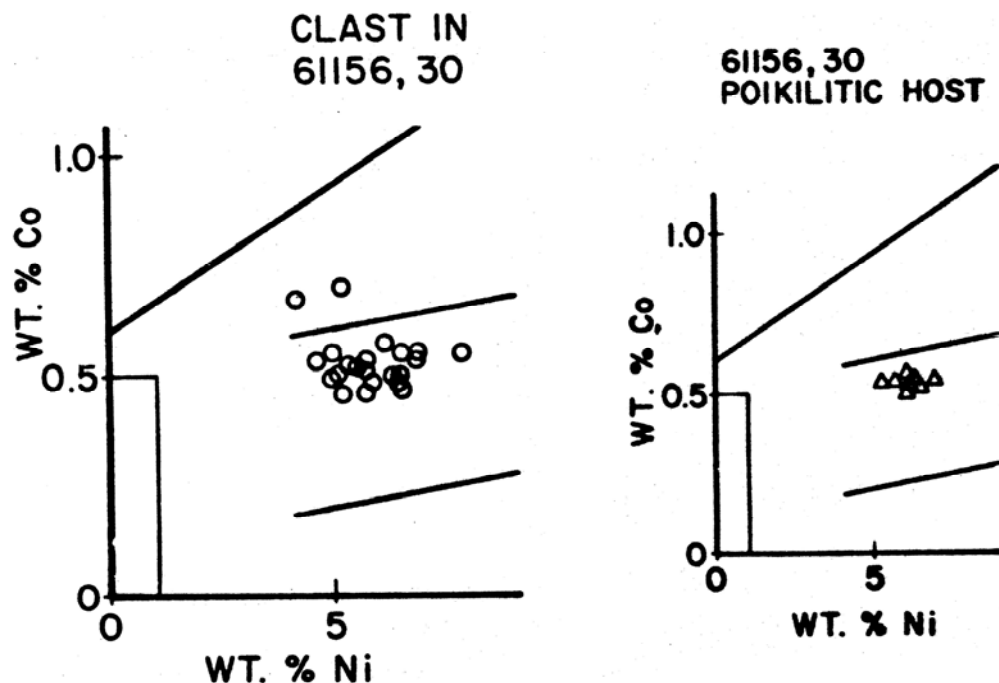


FIGURE 4. Metal compositions, from Hewins and Goldstein (1975a).

TABLE 3. Summary chemistry of 61156.

SiO ₂	45.0
TiO ₂	0.64
Al ₂ O ₃	23.0
Cr ₂ O ₃	0.13
FeO	7.8
MnO	0.11
MgO	9.7
CaO	13.5
Na ₂ O	0.40
K ₂ O	0.108
P ₂ O ₅	0.22
Sr	154
La	21.5
Lu	0.90
Rb	2.43
Sc	9.36
Ni	184-1190 (?)
Co	59.4
Ir ppb	23
Au ppb	22
C	
N	
S	1200
Zn	5.0
Cu	6.6

Oxides in wt% ; others in ppm except as noted.

PROCESSING OF SUBDIVISIONS: In 1972, 61156,0 was chipped to produce ,1 ,2 and ,4 from the N surface. In 1973, the largest piece remaining (61156,0) was entirely subdivided to produce ,3 and ,9-,13 (Fig. 7). ,9-,12 came from the W half of ,0. ,13 is the E end of ,0 and is now the largest single piece remaining (43.4 g). Other splits have since been made from the chips.

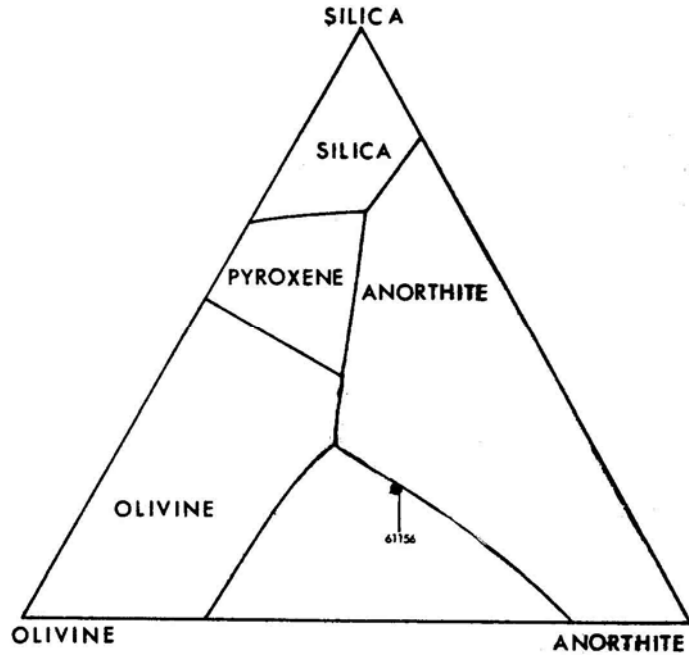


FIGURE 5. From Simonds et al. (1973).

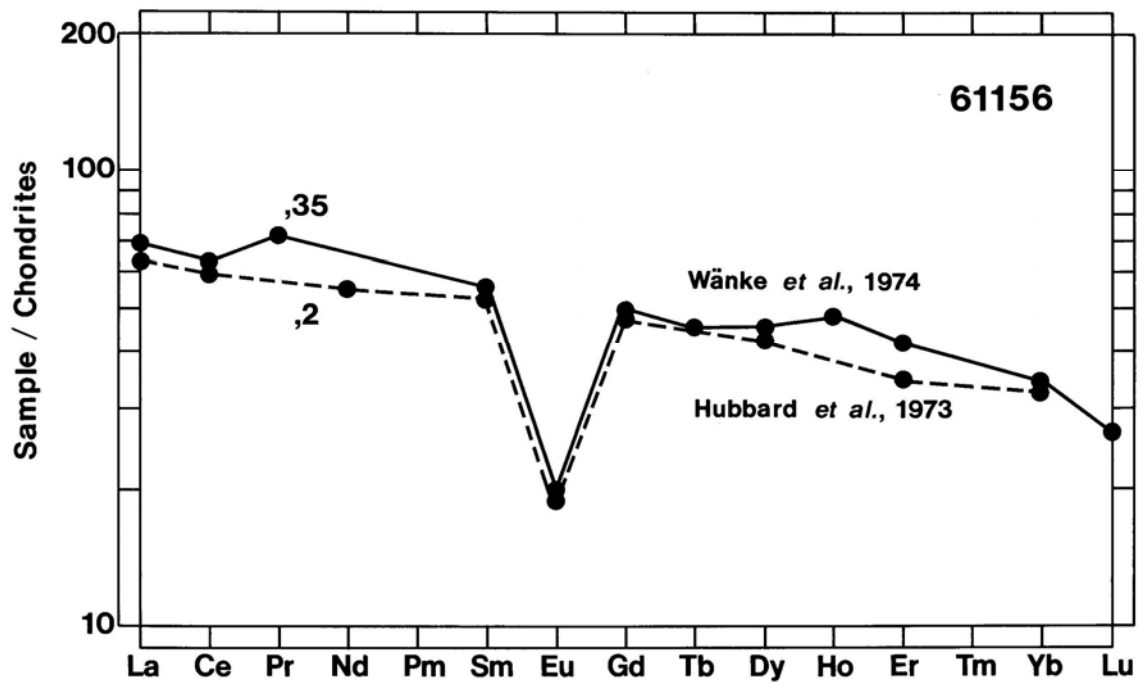


FIGURE 6. Rare earths.

TABLE 4. Summary of isotopic data on 61156.

$^{87}\text{Rb}/^{86}\text{Sr}$	$^{87}\text{Sr}/^{86}\text{Sr}$ measured	$^{87}\text{Sr}/^{86}\text{Sr}$ at 4.6 b.y.*	T_{BABI} (b.y.)	T_{LUNI} (b.y.)	Reference
0.0451	0.70202 \pm 8	0.69949	4.66 \pm .12		Tera <i>et al.</i> (1974)
0.0462 \pm 4	0.70217 \pm 5	0.69948	4.63 \pm .11	4.77 \pm .11	Nyquist <i>et al.</i> (1973)
*extrapolated from 3.9 to 4.6 b.y. and corrected for interlaboratory bias by Nyquist (1977)					
U-Th-Pb model ages (b.y.)					
$^{207}\text{Pb}/^{206}\text{Pb}$	$^{206}\text{Pb}/^{238}\text{U}$	$^{207}\text{Pb}/^{235}\text{U}$	$^{208}\text{Pb}/^{232}\text{Th}$	Reference	
4.24	4.21	4.23	3.88	Tera <i>et al.</i> (1974)	

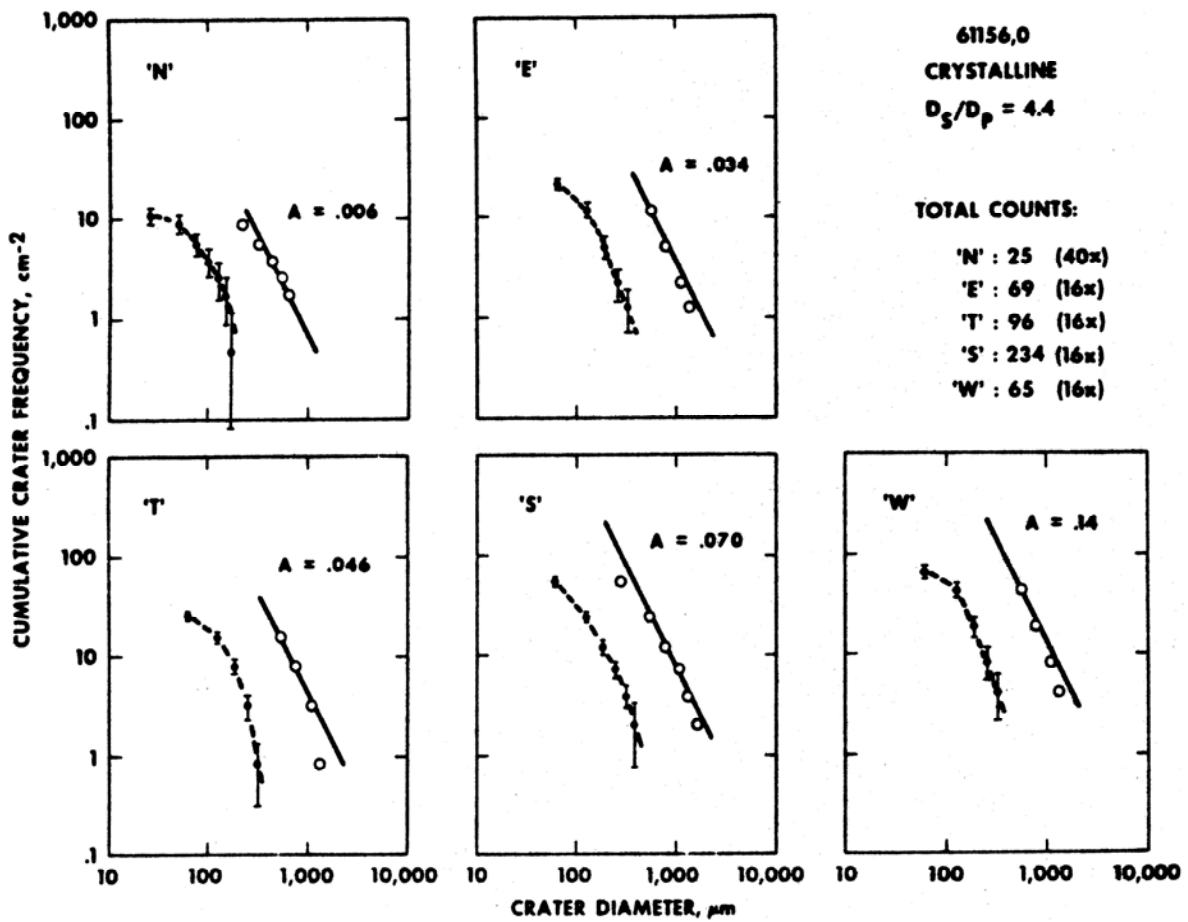


FIGURE 7. Microcraters, from Neukum *et al.* (1973).

TABLE 5. Distribution of Fe in the mineral phases of 61156*
(Huffman et al., 1974).

<u>Sample</u>	<u>pyroxene</u>	<u>olivine</u>	<u>ilmenite</u>	<u>troilite</u>	<u>metal</u>	<u>wt% metal</u>
61156,11	57.9	34.2	2.8	2.8	2.2	0.70
61156,12	49.3	43.9	2.0	1.8	2.9	1.76

*percentage of total Fe

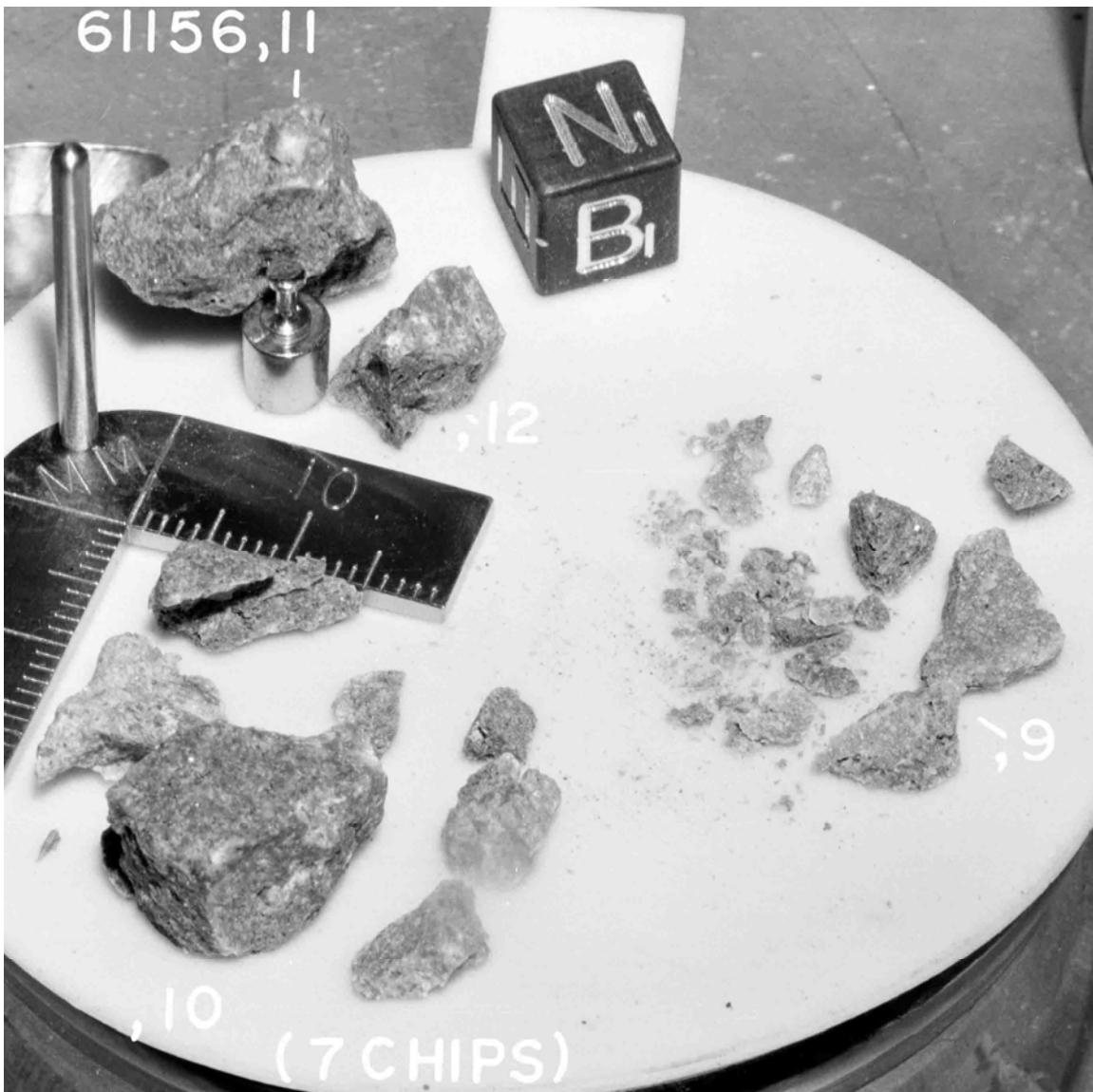


FIGURE 8. S-72-53534.